JOURNAL OF MATERIALS SCIENCE 32 (1997) 1563–1573

Fracture toughness evaluation of ductile polymeric films

S. HASHEMI
School of Polymer Technology, University of North London, Holloway Road, London N7 8DB, UK

The energy for complete fracture in double edge-notched tension test specimens has been measured for a wide range of polymer films. Results indicated that the variation of the total specific work of fracture, w_T, with ligament length, L, can be described by two straight lines, both of the form $w_T = w_e + \beta w_p L$, thus giving upper and lower intercept values at zero ligament length (i.e. w_e) for each film. The first term, w_e, is the energy absorbed per unit area of fracture, whereas the second term, w_p, is the energy absorbed per unit volume of plastic deformation remote from the fracture surface. The lower w_e value was obtained from the extrapolation of the data within the mixed mode region (plane-stress/plane-strain) where the maximum net-section stress exceeded 1.15 times that of the tensile yield stress, σ_y, of the material, and the upper value was ascertained by extrapolating the data within the plane stress region where the net-section stress was 1.15 σ_y. It appears that the transition from plane stress to plane strain mode of fracture in thin films occurs at a ligament length much greater than $5B$, where B is the specimen thickness. Moreover, it was found that the linearity of the data within the plane-stress region was not affected when ligament length values exceeded the plastic zone size. Moreover, variation of the extension to break with ligament length, for both pure plane stress and the mixed mode regions, was also linear; and the extrapolation values at zero ligament length were identified as crack opening displacements. Essential work estimated from the crack opening displacement agreed reasonably well with the extrapolated values.

1. Introduction

It is well established that fracture behaviour of polymers can be characterized either by the critical value of the stress intensity factor, K_c, or by the critical value of the J-integral, J_c. Both parameters are generally used in determining fracture toughness under plane strain which is independent of geometry and dimensions of the test piece. The plane-strain value of K_c or J_c is determined when some stringent specimen size criteria is adhered to. According to ASTM standards [1, 2], the validity of the measurements can only be ensured provided the specimen thickness, B, can satisfy the following size requirement for K_c and J_c testing, respectively

$$B_c \geqslant 2.5\left(\frac{K_c}{\sigma_y}\right)^2 \quad (1)$$

$$B_c \geqslant 2.5\left(\frac{J_c}{\sigma_y}\right) \quad (2)$$

The validity of both requirements, as represented by the above expressions, has been experimentally verified for a wide range of polymers [3–6] using specimen geometries such as compact tension (CTEN) and single edge-notched bend specimens (SENB). Results have shown that for high toughness and low yield-strength polymers, the thickness requirements could be quite large. However, for many applications such as packaging, polymers are used in thin-film forms with sub-millimetre thickness values. As it is impossible to test such films using CTEN or SENB geometries, the measured K_c or J_c are most likely to be invalid, because stipulated size requirements cannot be met. Recently, Hashemi and Yuan [7, 9] and Chan and Williams [10] have adopted an approach for characterizing polymeric films based upon Broberg's suggestion [11]. According to Broberg, the non-elastic region at the tip of a crack may be divided into two regions: an end region where the fracture process takes place, and the outer region where screening plastic deformation is necessary to accommodate the large strains in the end region (see Fig. 1). The total work of fracture can then be partitioned into two components: work that is expended in the fracture process to form a neck and subsequent tearing, and the work which is responsible for plastic deformation. The former is referred to as essential work and the latter as non-essential work. It is worth noting that this approach has been applied successfully to both metals [12–15] and polymers [16–19] in thin-sheet form. Again, as in K_c or J_c testing there are certain specimen size requirements that ought to be considered and these will be discussed in the following texts.

0022–2461

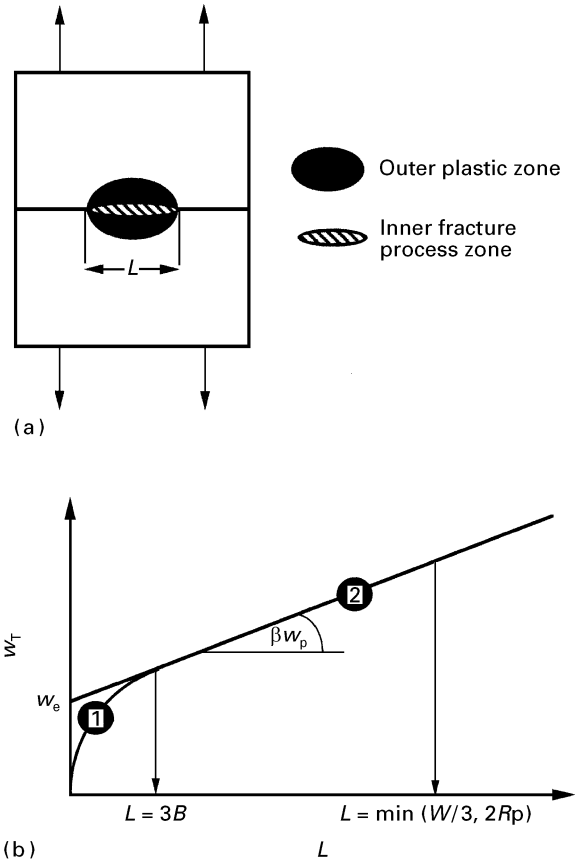

Figure 1 (a) Schematic diagram showing the fracture process zone and the outer plastic zone in DENT specimens. (b) Plot of specific total work of fracture, w_T, versus ligament length, L; (1) plane-stress/plane-strain, (2) plane-stress.

The aim of this paper is to verify the applicability of the above approach to characterize the fracture toughness of a range of polymeric films having different load–displacement characteristics.

2. Theory

The essential work approach divides the total input energy for fracture, W_T, into two components. The first component is the work that is expended in the fracture process zone, W_e, which is considered as being essential for the fracture process. This work is required to form a neck, which subsequently initiates tearing of the neck. The second component is work which is responsible for plastic deformation, W_p, but is not essential for fracture processes which, in the case of metals, involves shear and in the case of polymers involves micro-voiding and shear.

Note, the total work of fracture, W_T, as recorded during the mechanical test, contains all the energy dissipated during the test. For polymeric specimens this also includes the energy dissipated due to the viscoelastic nature of the material, W_v. Therefore, the total work of fracture may be written as

$$W_T = W_e + W_p + W_v \quad (3)$$

The above equation can be written as

$$w_T = \frac{W_T}{LB} = w_e + \frac{w_p V_p(L, B)}{LB} + \frac{W_v}{LB} \quad (4)$$

where $w_e = W_e/LB$, $w_p = W_p/BL^2$ and $V_p(L, B)$ is the volume of the plastic deformation zone. From our observations [20] on the plastic zone size, we can say that the volume $V_p(L, B)$ is proportional to BL^2 with a proportionality constant, β, that is independent of the ligament length, i.e.

$$V_p(L, B) = \beta L^2 B \quad (5)$$

Substituting Equation 5 into Equation 3 we obtain

$$w_T = w_e + \beta w_p L + \frac{W_v}{LB} \quad (6)$$

where w_e is termed the "specific essential work of fracture" and w_p is termed "the specific non-essential work of fracture". Assuming, however, that the viscoelastic energy term, W_v, is negligible, Equation 6 predicts a linear relationship between w_T and L having a positive intercept at $L = 0$ to give w_e, which is assumed to be a material property, and a slope that is proportional to w_p, as shown schematically in Fig. 1, i.e.

$$w_T = w_e + \beta w_p L \quad (7)$$

3. Specimen size criteria

It has been suggested that in order for W_T measurements to be considered valid, one has to satisfy the following conditions [12, 17].

Firstly, the ligament lengths used for extrapolation should be much longer than the specimen thickness to ensure that the material will always be in a state of pure plane stress. As the ligament length is reduced to values comparable to the sample thickness, the stress state will become mixed mode having both plane-stress and plane-strain character. In the mixed mode region the variation of w_T with ligament length often tends to be non-linear [17] as shown schematically in Fig. 1, thus suggesting that Equation 5 no longer applies. To prevent the onset of mixed-mode stress states, the essential work of fracture experiments are limited to ligament lengths that are greater than three to five times the sample thickness, i.e. $L > 3$–5B. This limitation can be experimentally checked by measuring the net-stress in the ligament at the point of full yielding. According to Hill [21], if σ_y is the yield stress of an unnotched specimen, then a fully yielded double edge-notched specimen in plane stress will yield at 1.15 σ_y while a specimen in plane strain will yield at 2.97 σ_y.

Secondly, the plastic zones at crack tips should overlap to ensure the ligament is fully yielded before the cracks start to grow thus maintaining the proportionality of W_p with L^2. This requires the ligament length to be smaller than twice the plastic zone radius, R_p, around a single crack tip.

Thirdly, the specimen width should be much larger than three times the ligament length so that yielding does not spread to the lateral boundary of the specimen, i.e. $L < W/3$.

The above restrictions on ligament length which, in effect, decide the dimensions of the test specimen, are generally expressed as

$$3B - 5B < \hat{L} \quad < \quad \min(W/3, 2R_p) \tag{8}$$

where $2R_p$ may be estimated from linear elastic fracture mechanics. For a circular plastic zone, $2R_p$ can be estimated from

$$2R_p \quad = \quad \frac{Ew_e}{\pi\sigma_y^2} \tag{9}$$

and for a line plastic zone from

$$2R_p \quad = \quad \frac{\pi Ew_e}{8\sigma_y^2} \tag{10}$$

where E is the tensile modulus and σ_y is the tensile yield stress of the material.

4. Experimental procedure

4.1. Materials

A wide range of commercially available polymer films was used in this study as delineated in Table I. Films were received in the form of A4 size sheets of thicknesses specified in Table I. The way in which the films were fabricated and their morphological specifications are discussed below.

4.2. Tensile tests

Four dumb-bell shaped specimens were tested for each material in simple extension on an Instron testing machine at a constant crosshead speed of 2 mm min^{-1}. A load–displacement diagram for each specimen was recorded and the tensile yield stress was evaluated. For materials in which there was no distinct yield point, the yield stress was taken at a 0.2% strain offset, whereas for the other materials it was taken as the maximum stress measured. Schematic representation of typical load–displacement diagrams is shown in Fig. 2.

4.3. Fracture tests

Rectangular coupons, 50 mm wide and 110 mm long, were cut from the films such that their lengths

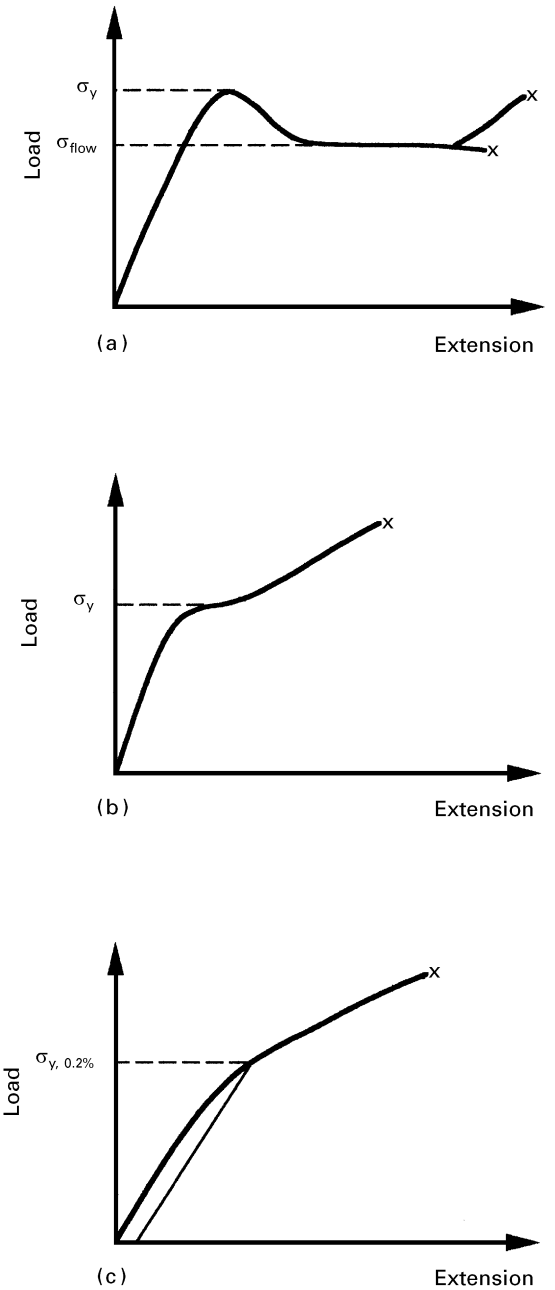

Figure 2 Schematic representation of typical tensile load–displacement diagrams observed in this study. (a) PEEK, PC, PBT, PEI and CA films; (b) PET (SWC, MX400, HOSTAPHAN) and PI films; (c) PET (329, 377) and PEN films.

TABLE I Materials

Materials	Trade name	Supplier	B (μm)
Polyethylene terephthalate (PET) (polyester)			
Grades:	Melinex 377	ICI	125
	Melinex 329	ICI	125
	Melinex SWC	ICI	125
	Melinex MX400	ICI	125
	Hostaphan	Hoechst	125
Polyethylene naphthalate (PEN)	Kaladex 2000	ICI	125
Poly(ether-ether ketone) (PEEK)	Stabar K200	ICI	125
Polycarbonate (PC)	Makrofol DE	Bayer	125
Polybutylene terepthalate (PBT)	Valox FR-1	GE	125
Cellulose acetate (CA)	Clarifoil	Courtaulds	125
Polyetherimide (PEI)		GE	125
Polyimide (PI)	Upilex R	ICI	125

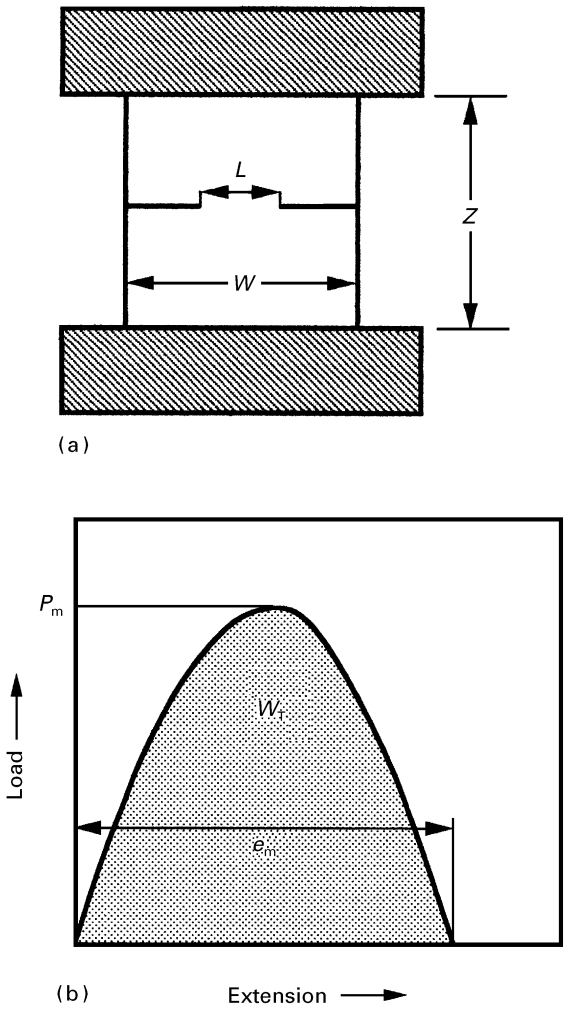

Figure 3 Specimen geometry and the measured quantities.

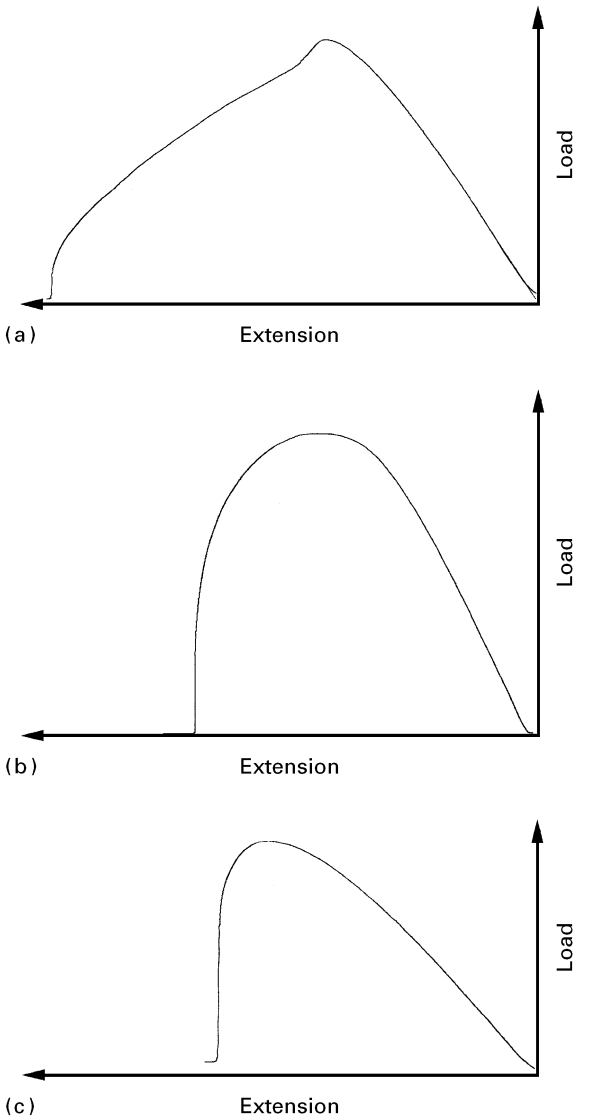

Figure 4 Typical DENT load–displacement diagrams observed in this study: (a) PEEK, PBT, PC; (b) PET; (c) PEN, PEI, PI and CA films.

were always perpendicular to the machine direction. Double edge-notched tension (DENT) type test pieces (see Fig. 3) were then prepared by razor notching the coupons to various a/W values giving ligament lengths ranging from 3–17 mm ($L \leqslant W/3$ in order to avoid edge effects [12, 17]). DENT specimens were then tested on an Instron tensile testing machine at a constant displacement rate of 2 mm min^{-1} using pneumatic clamps with gauge length, Z, of 50 mm. Load–displacement diagram for each test was recorded, from which the maximum load, P_m, maximum extension to break, e_m, and the total fracture energy, W_T, were measured as depicted in Fig. 3. Examples of typical load–displacement diagrams obtained during the course of this study are shown in Fig. 4.

5. Results and discussion

5.1. Work of fracture

5.1.1. Poly(ethylene terephthalate), PET films

As indicated in Table I, five grades of polyester films were used in this investigation. The Melinex films provided by ICI were all biaxially oriented. Grade 377 is a matt-surfaced translucent white film, 329 is a high opacity pearly white film with a satin surface finish, SWC is a slightly hazy film and MX400 is a sparkling clear film. The Hostaphan film supplied by Hoechst was a hazy, biaxially oriented and heat-set film. The unnotched tensile load–displacement diagrams for SWC, MX400 and Hostaphan showed a clear yield point, whereas for 329 and 377 the 0.2% strain offset was needed to determine the yield stress. Tensile yield stress values are given in Table II.

Fig. 4 depicts a DENT load–displacement diagram which exemplifies the behaviour of these films. This trace and many others obtained during the course of this study indicate that PET films fail by ductile tearing. In all the films, the onset of slow stable crack propagation occurred before the maximum load was reached. The plastic deformation zone that was developed at each notch tip, was not clearly visible as indicated by the example shown in Fig. 5. However, close examination of the specimens suggested a circular plastic zone which had almost the same opacity as that of the bulk material, hence making it difficult to identify. Because of this, one could not establish visually whether the complete ligament yielding occurred at or prior to attaining the maximum load. However, as shown in Figs 6–10, plots of the maximum net-section stress, σ_n (maximum load divided by the

TABLE II Fracture data for PET films

Grade	σ_y (MPa)	w_e (kJ m^{-2})	βw_p (MJ m^{-3})	w_e^{*a} (kJ m^{-2})	βw_p^{*a} (MJ m^{-3})	A	n
377	100	68.49	7.06	48.41	10.65	46.10	0.49
SWC	97.37	65.70	8.93	48.60	11.46	43.95	0.55
MX400	98.64	65.43	7.32	47.78	10.02	43.09	0.51
329	87	55.82	5.56	45.01	07.37	37.36	0.48
Hostaphan	100	53.66	5.96	36.06	07.88	30.70	0.57

[a] Values obtained using the data in the mixed mode region.

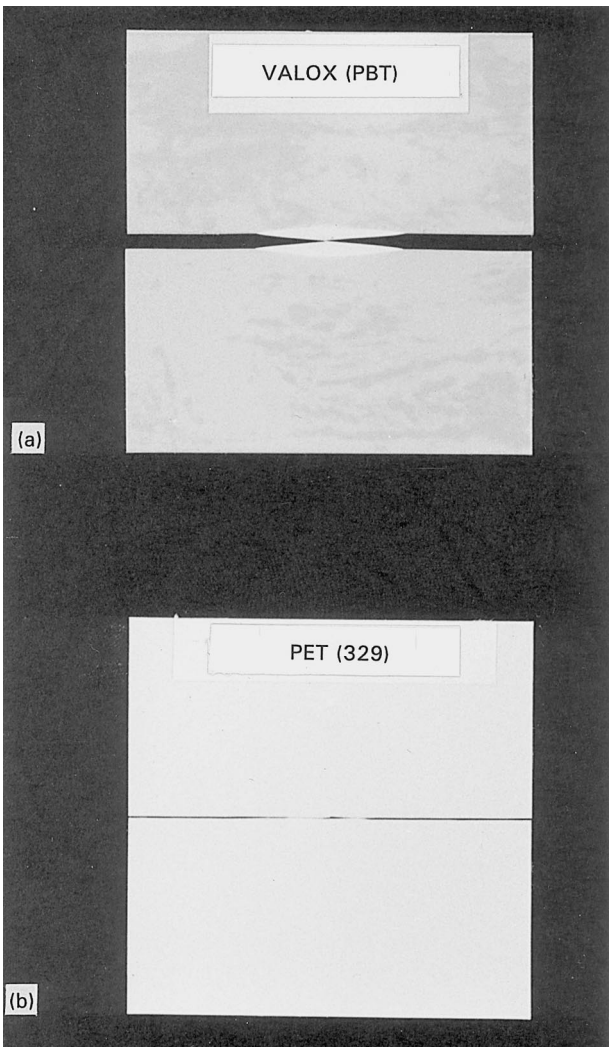

Figure 5 Fractured specimens: (a) typical of PBT, PEEK, PC, PEI, PI and CA films; (b) typical of PET and PEN films.

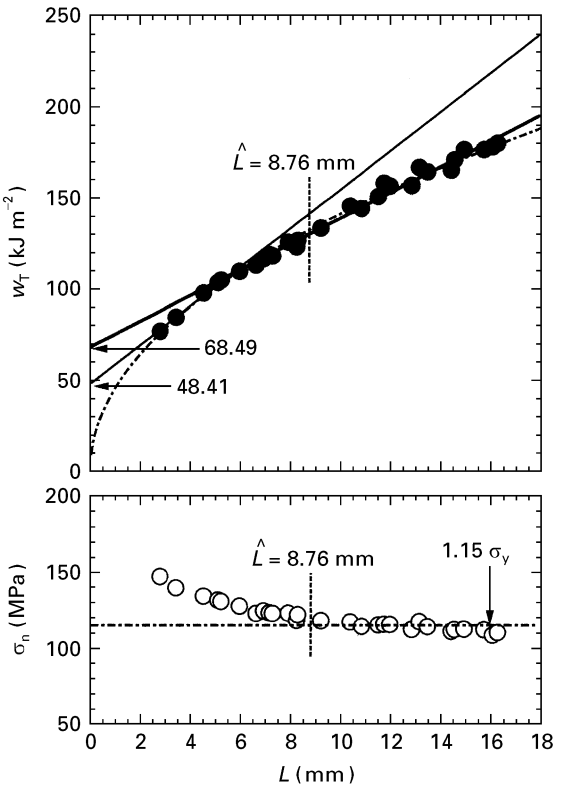

Figure 6 Plots of specific total work of fracture and the maximum net-section stress versus ligament length for PET/377.

original ligament length and thickness), as a function of ligament length, indicate that for long ligament lengths, the maximum net-section stress is constant and is close to 1.15 σ_y as predicted by Hill [21]. For short ligament lengths, σ_n values exceeded 1.15 σ_y thus suggesting a mixed mode stress state. It can be seen that for each material the onset of mixed mode stress occurs at a ligament length value far greater than 5B which for a thickness of 0.125 mm it should correspond to 0.625 mm.

Also shown in Figs 6–10 are the corresponding plots of the total specific work of fracture, w_T, versus ligament length, L, for the five PET films. As can be seen, the data span a range of ligament lengths from well within the mixed-mode region where $\sigma_n > 1.15\ \sigma_y$ to the pure plane-stress region where $\sigma_n = 1.15\ \sigma_y$. Evidently, those specimens within the mixed mode region fracture at lower w_T values than those within the pure plane-stress region. It is worth noting that the data within each region vary linearly with ligament length. By extrapolating the specific work of fracture of the pure plane-stress samples and those of mixed mode samples to zero ligament length, values of the pure plane stress and the plane-strain essential work of fracture were determined. These values are given in Table II as w_e and w_e^*, respectively. Also given in the table are the respective values of the non-essential work of fracture, i.e. βw_p and βw_p^*, determined from the slope of these lines. It is worth noting that the heat-set (Hostaphan) and the satin finish (Melinex 329) films gave similar energy values; but the values of both these films were lower than that of untreated films.

Using the plane-stress specific essential work of fracture and the Young's modulus value of 4 GPa, the maximum ligament length, $\hat{L}$, for complete ligament

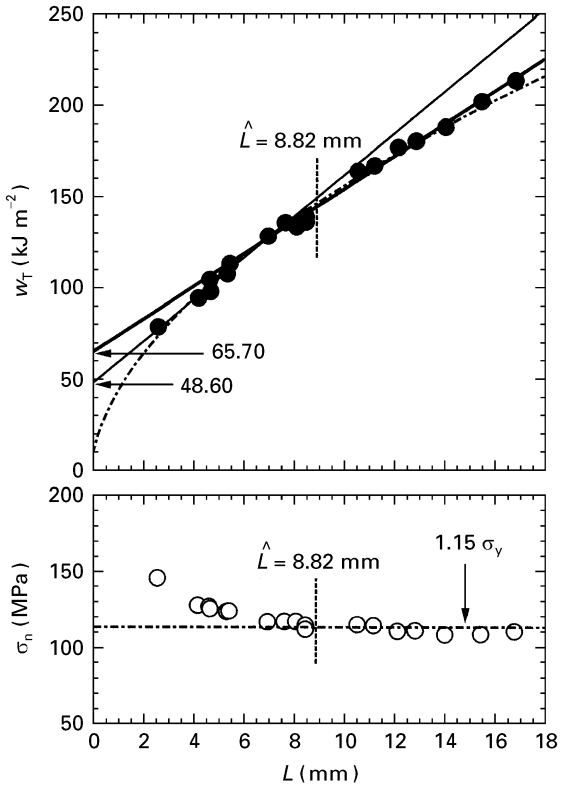

Figure 7 Plots of specific total work of fracture and the maximum net-section stress versus ligament length for PET/SWC.

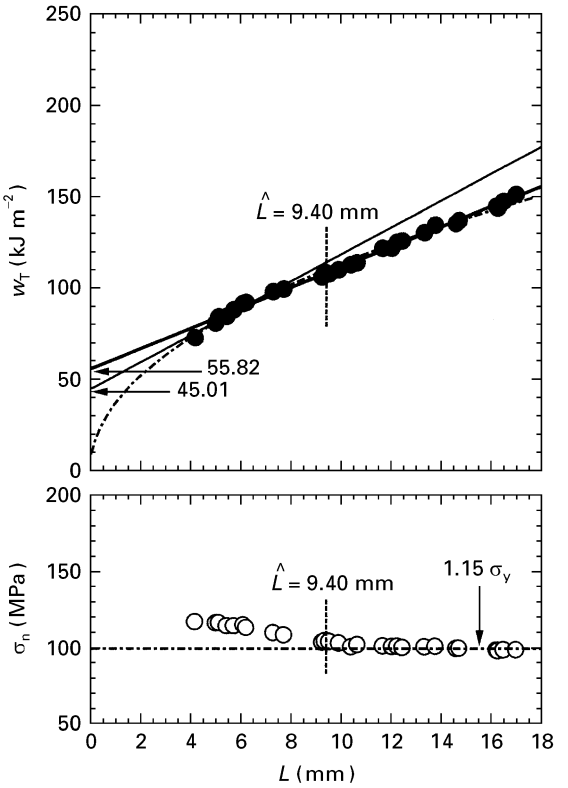

Figure 9 Plots of specific total work of fracture and the maximum net-section stress versus ligament length for PET/329.

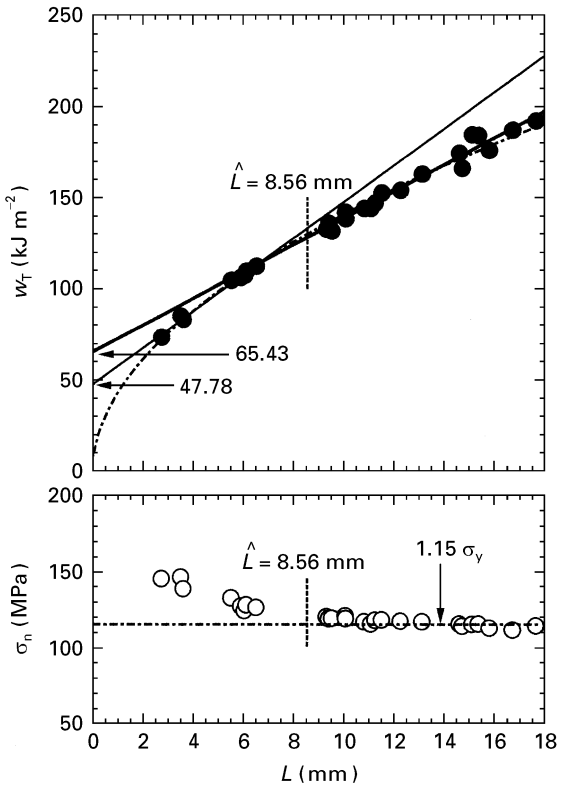

Figure 8 Plots of specific total work of fracture and the maximum net-section stress versus ligament length for PET/MX400.

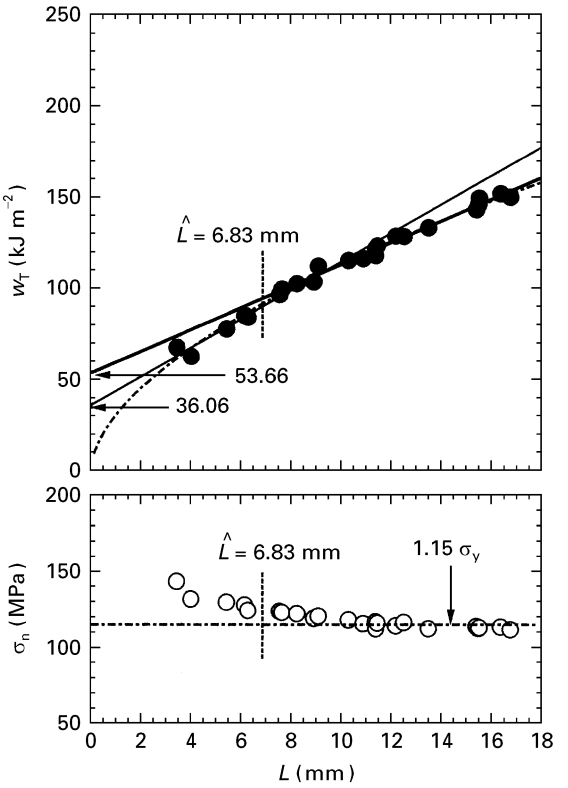

Figure 10 Plots of specific total work of fracture and the maximum net-section stress versus ligament length for PET/Hostaphan.

yielding was estimated for each material according to Equation 9 and displayed in Figs 6–10 as dotted lines. It should be noted that the linearity of the data within pure plane-stress region was still maintained, even though for the majority of the specimens the ligament length values exceeded $\hat{L}$, thus suggesting that, despite failing to satisfy the condition that the ligament length should be less the plastic zone size, the proportionality of w_p with L^2 is still maintained.

The resemblance of w_T versus L plots with the J-integral versus crack extension plots suggest that a power law relation of the form

$$w_T = AL^n \quad (11)$$

should also describe the variation of total specific work of fracture with ligament length. As shown in Figs 6–10, the power-law relation fits the data through both the mixed-mode regions and the pure plane stress region reasonably well. However, as stated by Saleemi and Narin [17], although Equation 11 can correlate the data, it has no theoretical basis and it cannot be used to determine the specific essential work of fracture by extrapolation to zero ligament length. Moreover, it is also difficult to justify the choice of any particular ligament length for proposing a failure criterion based on the value of the specific work of fracture at some specified ligament length. Nevertheless, the power-law relation is a useful means by which materials could be compared. Values of A and n for all PET films are also listed in Table II for comparison purposes.

5.1.2. PC, PBT and PEEK films

The unnotched tensile load–displacement diagrams for all three films showed a clear yield point after which all three materials sustained a constant stress, σ_{flow}, before failure, as shown schematically in Fig. 2. Fig. 4 depicts a DENT load–displacement diagram which exemplifies the behaviour of these films. As can be seen, the behaviour is indicative of ductile failure with slow stable crack growth. Crack growth was accompanied by progressive development of a yielded zone ahead of the crack tips. At maximum load, the two plastic deformation zones overlapped, causing complete ligament yielding and a momentary drop in load. The initial notches continued to grow stably within the overlapped deformation zone until they eventually met half way along the ligament length causing complete failure of the test specimens. Fig. 5 shows a photograph of two halves of a PBT specimen at fracture; as can be seen, the plastic deformation zone at fracture can be identified as a diamond-shaped zone. A similar plastic deformation zone was observed in PC and PEEK specimens.

Figs 11–13 show plots of the maximum net-section stress, σ_n, as a function of ligament length. These plots indicate that for long ligament lengths, the maximum net-section stress is constant and is close to 1.15 σ_u, where σ_u is taken as 1/2 ($\sigma_y + \sigma_{flow}$) as shown in Fig. 4. For short ligament lengths, σ_n values exceeded 1.15 σ_y, thus suggesting a mixed mode stress state. It can be seen that for each material the onset of mixed mode stress again occurs at a ligament length value far greater than 5B. Figs 11–13 also show the corresponding plots of the total specific work of fracture, w_T, versus ligament length, L. Once again, specimens within the mixed mode region fracture at lower w_T values than those within the pure plane-stress region. Values of the pure plane-stress and the plane-strain essential and non-essential works of fracture are given in Table III. The maximum ligament length, $\hat{L}$, for

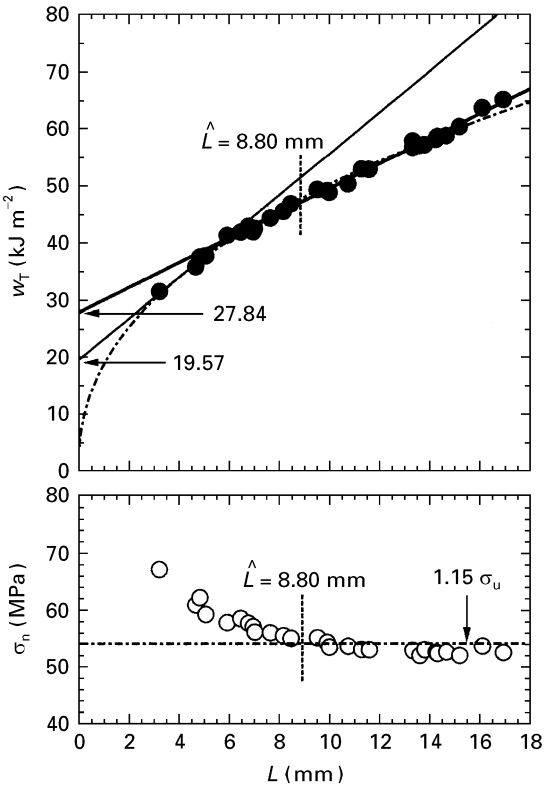

Figure 11 Plots of specific total work of fracture and the maximum net-section stress versus ligament length for PC.

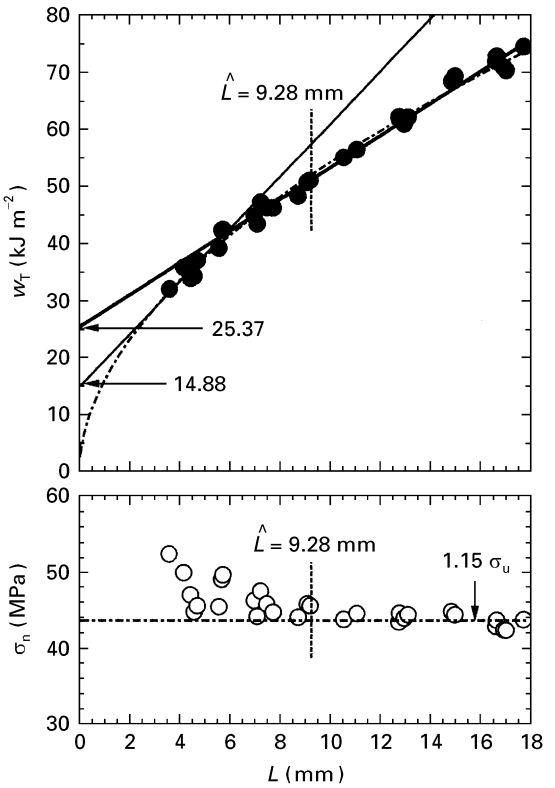

Figure 12 Plots of specific total work of fracture and the maximum net-section stress versus ligament length for PBT.

complete ligament yielding was estimated using Equation 10. These values are shown as dotted lines in Figs 11–13 where it can be seen that again the linearity of the data was still maintained even though the ligament length values exceeded $\hat{L}$.

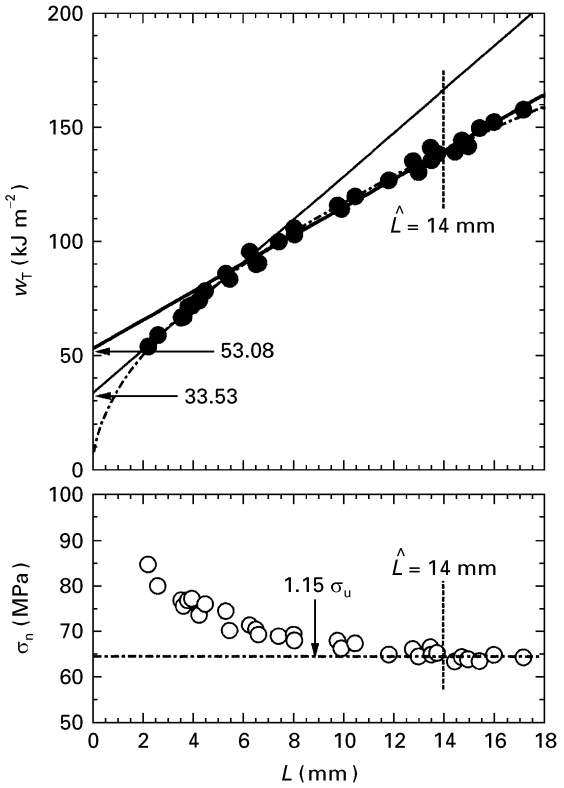

Figure 13 Plots of specific total work of fracture and the maximum net-section stress versus ligament length for PEEK.

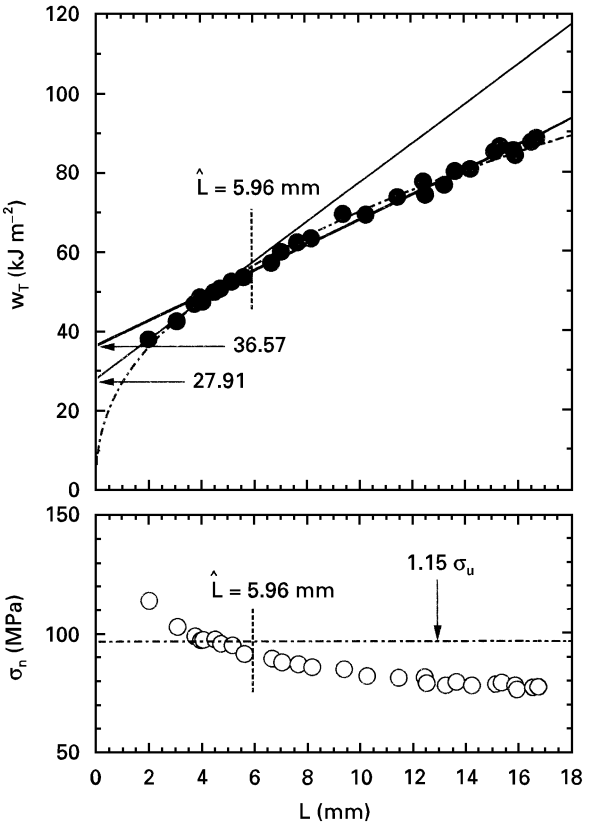

Figure 14 Plots of specific total work of fracture and the maximum net-section stress versus ligament length for PEI.

The power-law relation also fits the data through both the mixed mode regions and the pure plane-stress region reasonably well. Curve fitting of parameters A and n is also given in Table III.

It is noteworthy that the essential and non-essential work of fracture for PEEK film is much higher than those of PC and PBT films; mainly because its extension to break values were considerably greater. In fact, values of the essential and non-essential work of fracture for PEEK are very similar to the values obtained for PET/329 and PET/Hostaphan. Although PET films are much stronger, the extension to break for PEEK film is much greater.

5.1.3. Polyimide (PI), polyetherimide (PEI), poly(ethylene naphthalate) (PEN) and cellulose acetate (CA)

The unnotched tensile specimens of PEI, PI and CA materials showed a clear yield point, but those of PEN showed no clear yield point. For this material the yield stress was taken at a 0.2% strain offset. The notched DENT specimens for all four materials gave load–displacement diagrams similar to that shown schematically in Fig. 4. The plastic deformation zone that was developed at each notch tip was clearly visible in PEI, CA and PI films and had a diamond-shaped appearance at fracture. However, the plastic zone in PEN film was not as clearly defined as in PET films because it had the same opacity as that of the bulk material. In these materials, slow stable crack propagation occurred before maximum load was reached. When the two plastic deformation zones overlapped, the crack at each notch tip propagated rapidly through the overlapped zone in an unstable fashion. Plots of σ_n and w_T versus ligament length for all four materials are shown in Figs 14–17. Clearly, the maximum net-section stress for long ligament lengths is well below 1.15 σ_y, mainly because for long ligament lengths complete ligament length yielding occurred after the maximum load. However, as shown in Figs 14–17, variation of w_T with ligament lengths is similar to the other materials, showing two possible extrapolations to zero ligament length. Results obtained from these extrapolations are given in Table IV together with the power-law fit of parameters A and n.

TABLE III Fracture data for PC, PBT and PEEK films

Material	σ_u (MPa)	E (GPa)	w_e (kJ m^{-2})	βw_p (MJ m^{-3})	w_e^* (kJ m^{-2})	βw_p^* (MJ m^{-3})	A	n
PC	46.96	2.30	27.84	2.18	19.57	3.63	18.73	0.43
PBT	37.96	1.50	25.37	2.80	14.90	4.63	16.06	0.53
PEEK	55.75	2.50	53.08	6.20	33.53	9.55	34.86	0.53

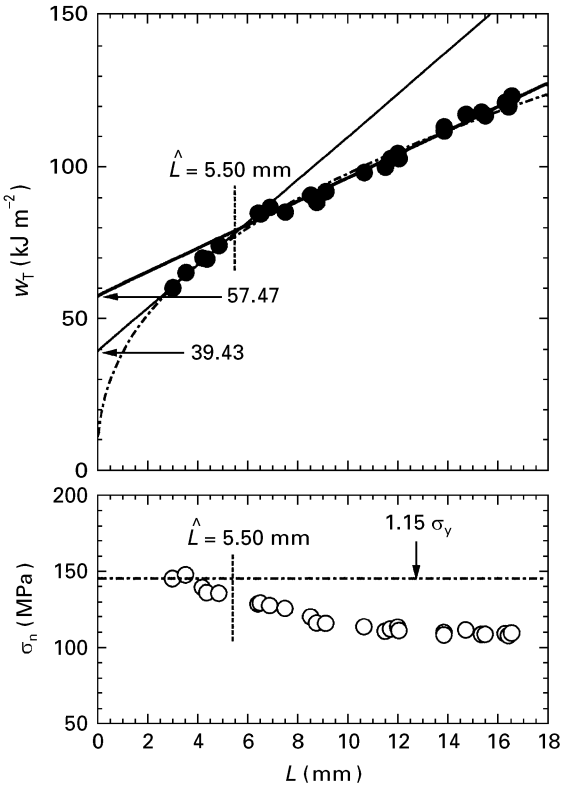

Figure 15 Plots of specific total work of fracture and the maximum net-section stress versus ligament length for PI.

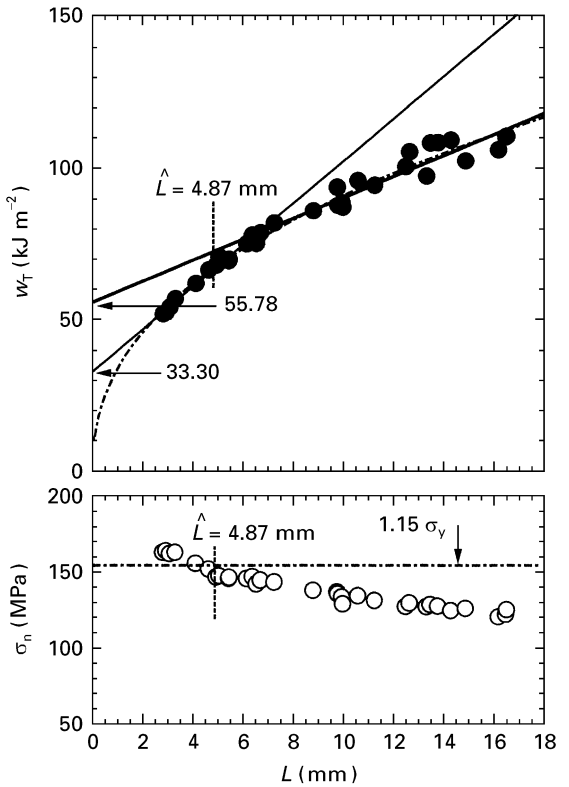

Figure 16 Plots of specific total work of fracture and the maximum net-section stress versus ligament length for PEN.

5.2. Crack opening displacement

Fig. 18 shows some selected plots of maximum extension (i.e. at break), e_m, measured from load–displacement diagrams versus ligament length. Apparently, the data within pure plane stress and within the mixed

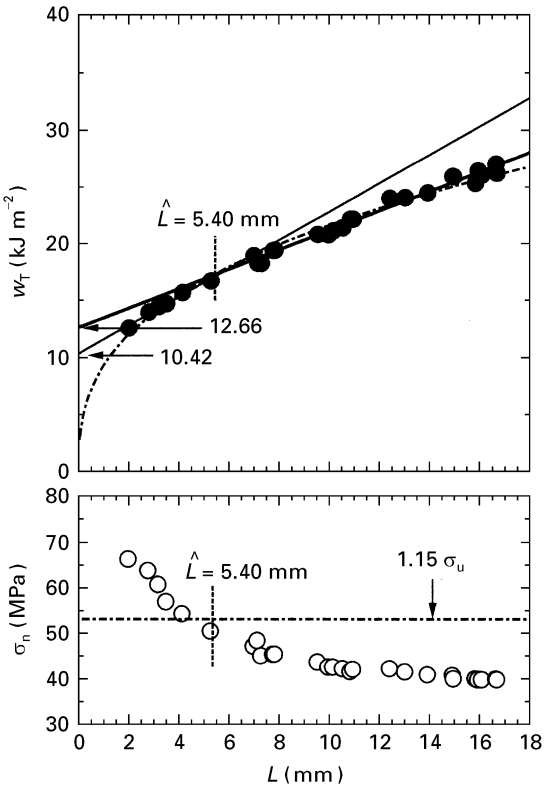

Figure 17 Plots of specific total work of fracture and the maximum net-section stress versus ligament length for CA.

regions each follow a straight line relationship similar to Equation 7 with a positive intercept, e_0, for pure plane-stress and e_0^* for the mixed mode regions, i.e.

$$e_m = e_0 + e_p L \quad (12)$$

The positive intercepts suggests that some of the plastic deformation must have been directly associated with fracture and are not related to the ligament length. The intercept, e_0, has been identified with the critical crack opening displacement [11, 16] and its values for different materials used in this work are given in Table V. With regard to possible relationship between e_0 and w_e, a similar relationship has already been proposed by Wells [22] between G_c and the crack opening displacement, δ, i.e.

$$G_c = \delta\sigma_y \quad (13)$$

As mentioned earlier, it is reasonable to anticipate that when ligament length approaches zero, e_0 approximates to δ and w_e to G_c, i.e.

$$w_e = e_0\sigma_y \quad (14)$$

(or alternatively $w_e = e_0\sigma_u$). Similarly, one may anticipate that when ligament length approaches zero, e_0^* approximates to δ^* and w_e^* to G_c^* where G_c^* is the plane-strain value of G_c. Estimated values of w_e and w_e^* are given in Table V and compared with the direct measurements. Considering that e_0 and e_0^* values were obtained from elongations of entire specimens rather than using a clip gauge across the plastic deformation zones (difficult to use anyway because of the thickness of the films), the agreement between the measured and the estimated values is reasonably good.

TABLE IV Fracture data for PEI, PI, PEN and CA films

Material	σ_u (MPa)	E (GPa)	w_e (kJ m^{-2})	βw_p (MJ m^{-3})	w_e^* (kJ m^{-2})	βw_p^* (MJ m^{-3})	A	n
PEI	85.05	3.01	36.57	3.16	27.91	4.94	26.84	0.42
PI	125[a]	3.80	57.47	3.88	39.43	7.07	38.83	0.40
PEN	135[a]	5.01	55.78	3.46	33.30	7.00	34.51	0.42
CA	46.08	2.30	12.66	0.85	10.42	1.24	09.41	0.36

[a] Yield stress values.

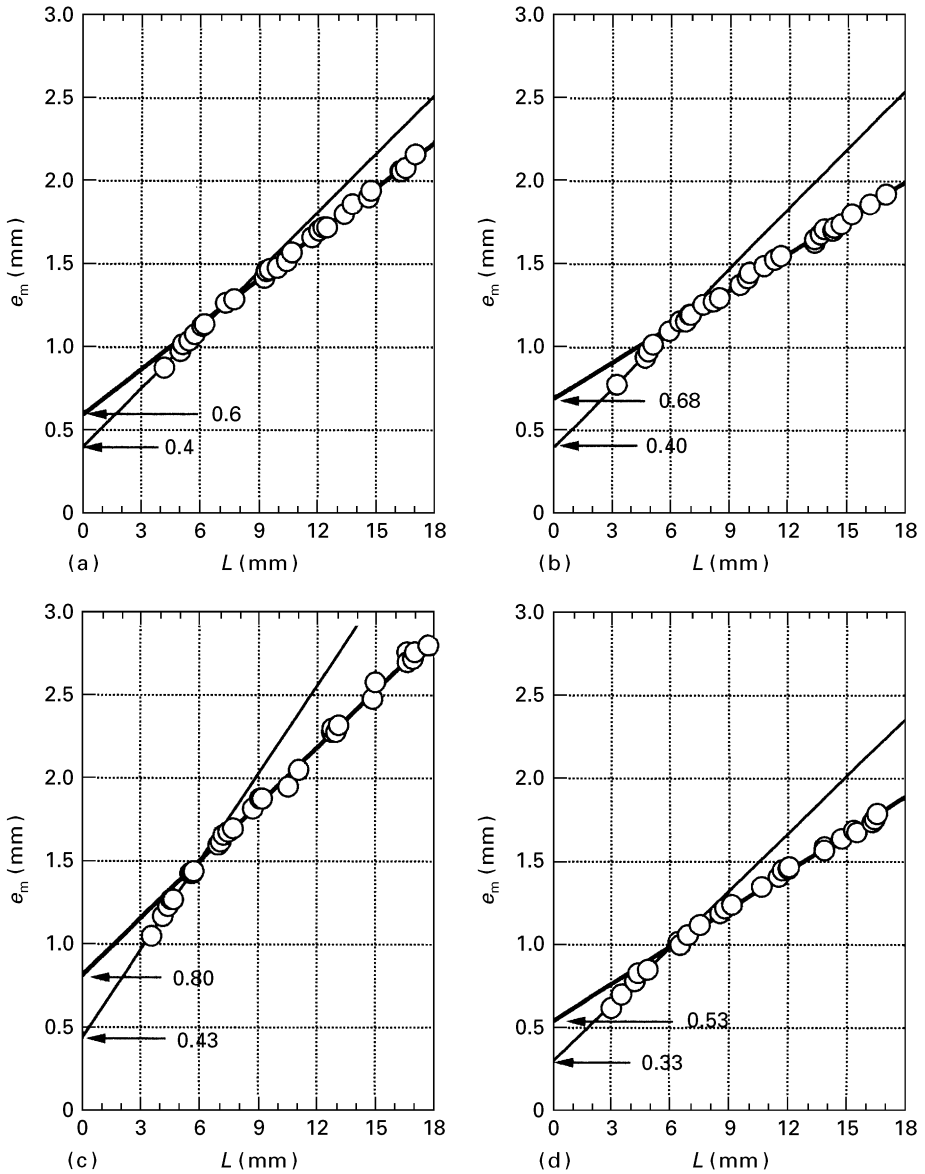

Figure 18 Typical plots of extension to break versus ligament length: (a) PET/329, (b) PC, (c) PBT, (d) PI.

6. Conclusion

It has been shown that for a wide range of polymeric films the variation of specific total work of fracture within the plane-stress region is a linear function of the ligament length. It was noted that the transition from a pure plane-stress region when the net section stress, σ_n, is 1.15 σ_y to a mixed mode region when $\sigma_n > 1.15$ σ_y occurs at ligament length values much greater than $5B$. Variation of the specific total work of fracture with ligament length was still reasonably linear within the mixed mode region. It has also been shown that the linearity of the data within the pure plane stress region was not affected when ligament length values exceeded the plastic zone size. Moreover, variation of the extension to break with ligament length for both pure stress and the mixed mode regions was also linear and the extrapolation values at zero ligament length were identified as crack opening displacement. Essential work estimated from the crack opening displacement agreed reasonably well with the direct measurement.

TABLE V Crack opening displacement

Grade	Estimated				Measured
	e_0 (mm)	w_e (kJ m^{-2})	e_0^{*a} (mm)	w_e^{*a} (kJ m^{-2})	w_e, w_e^{*a} (kJ m^{-2})
PET/377	0.60	60.00	0.40	40.00	68.49, 48.41
PET/SWC	0.60	58.42	0.41	39.92	65.70, 48.60
PET/MX400	0.64	63.13	0.39	38.47	65.43, 47.78
PET/329	0.60	52.20	0.40	34.80	55.82, 45.01
PET/HOSTA	0.51	51.00	0.33	33.00	53.66, 36.06
PC	0.68	31.93	0.40	18.78	27.84, 19.57
PBT	0.80	30.37	0.43	16.32	25.37, 14.88
PEEK	0.98	54.75	0.49	27.32	53.08, 33.53
PEI	0.48	40.82	0.33	28.07	36.57, 27.91
PI	0.53	66.25	0.30	37.50	57.47, 39.43
PEN	0.38	51.30	0.22	29.70	55.78, 33.30
CA	0.30	13.82	0.20	09.22	12.66, 10.42

[a] Values obtained from the extrapolation of the data within the mixed mode regions.

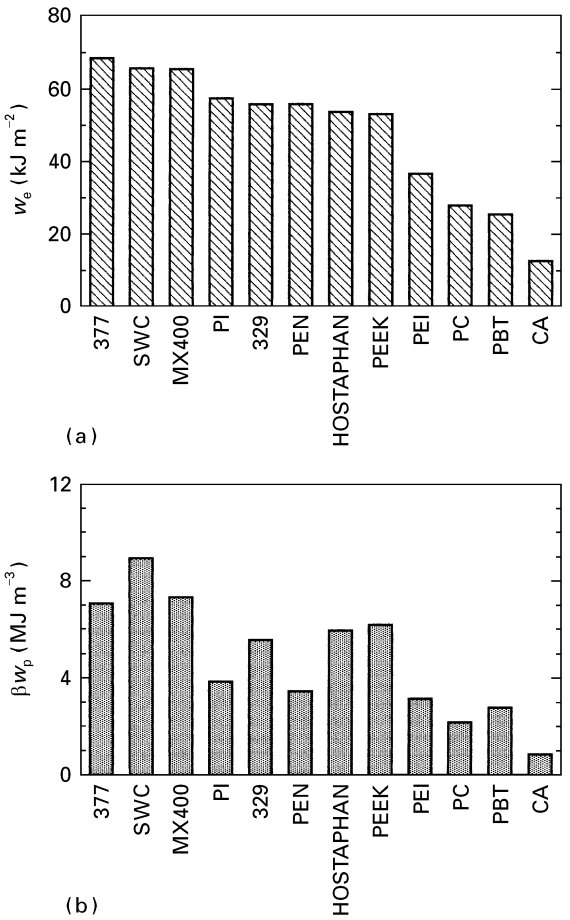

Figure 19 Bar charts comparing (a) w_e values and (b) βw_p values of the films studied in this work.

Bar charts presented in Fig. 19a and b compare w_e and βw_p values for the films tested in this work. As can be seen, for the majority of the films, the pure plane-stress specific essential work of fracture falls within the range 53–68 kJ m^{-2}. This range includes PET, PEN, PI and PEEK films. For PC, PBT and PEI films it fell within the range 25–40 kJ m^{-2}. CA film gave the lowest energy of all the films tested in this work (13 kJ m^{-2}). The specific non-essential work of fracture was highest for PET and PEEK films with values around 7 MJ m^{-3} and was lowest for CA film with a value of 0.85 MJ m^{-3}. For the rest of the materials it was in the range 2–4 MJ m^{-3}.

Acknowledgements

The author thanks Bayer, GE plastics, Hoechst, ICI and Courtaulds for supplying the films.

References

1. W. F. BROWN and J. SRAWLEY, ASTM STP 410 (American Society for Testing and Materials, Philadelphia, PA, 1966).
2. J. D. LANDES and J. A. BEGLEY, ASTM STP 560 (American Society for Testing and Materials, Philadelphia, PA, 1974) p. 170.
3. S. HASHEMI and J. G. WILLIAMS, *J. Mater. Sci.* **19** (1984) 3746.
4. *Idem*, *Polymer* **27** (1986) 382.
5. *Idem*, *J. Polym. Eng. Sci.* **26** (1986) 760.
6. P. L. FERNANDO and J. G. WILLIAMS, *ibid.* **20** (1980) 215.
7. S. HASHEMI and Z. YUAN, *J. Plast. Rubb. Compos. Process. Applic.* **21** (1994) 151.
8. S. HASHEMI, *ibid.* **20** (1993) 229.
9. S. HASHEMI and D. O'BRIEN, *J. Mater. Sci.* **28** (1993) 3977.
10. W. F. CHAN and J. G. WILLIAMS, *Polymer* **35** (1994) 1666.
11. K. B. BROBERG, *Int. J. Fract.* **4** (1968) 11.
12. B. COTTERELL and J. K. REDDEL, *ibid.* **13** (1977) 267.
13. Y. W. MAI and B. COTTERELL, *J. Mater. Sci.* **15** (1980) 2296.
14. *Idem*, *Eng. Fract. Mech.* **21** (1985) 123.
15. M. P. WUNK and D. T. REED, *Int. J. Fract.* **31** (1986) 161.
16. C. A. PATON and S. HASHEMI, *J. Mater. Sci.* **27** (1992) 2279.
17. A. S. SALEEMI and J. A. NARIN, *J. Polym. Eng. Sci.* **30** (1990) 211.
18. Y. W. MAI and P. POWELL, *J. Polym. Sci. Polym. Phys. Edn* **29** (1991) 785.
19. Y. W. MAI and B. COTTERELL, *Int. J. Fract.* **32** (1986) 2296.
20. S. HASHEMI, to be published.
21. H. HILL, *J. Mech. Phys. Solids* **4** (1952) 19.
22. A. A. WELLS, *Br. Weld. J.* **10** (1963) 563.

Received 31 October
and accepted 1 December 1995